Int. J. Electrochem. Sci., 11 **(2016)** 1 - 13

International Journal of ELECTROCHEMICAL SCIENCE
www.electrochemsci.org

Characterization of Intergranular Stress Corrosion Cracking of 304 Stainless Steel by Electrochemical Noise and Acoustic Emission Techniques

Bo Li[1,2], *JihuiWang*[1,2,*], *XuehuiWang*[2], *Xin Yue*[2]

[1] State Key Laboratory of Hydraulic Engineering Simulation and Safety, Tianjin University, Tianjin 300072, P R China
[2] Tianjin Key Laboratory of Composite and Functional Materials, School of Materials Science and Engineering, Tianjin University, Tianjin 300072, P R China
[*]E-mail: jhwang@tju.edu.cn

Received: 14 August 2015 / *Accepted:* 2 September 2015 / *Published:* 1 December 2015

The intergranular stress corrosion cracking of sensitized 304 stainless steel in $Na_2S_2O_3$ solutionwas detected by electrochemical noise (EN) and acoustic emission (AE) techniques. The parameters of noise resistance (R_n), standard deviation (S_I) and wavelet fractal dimension (D) were determined from EN data, and *K*-means cluster and correlation methods were used to characterize the AE data. The results show thatin the elastic deformation process the small transients in EN and low amplitude of AE hits are related to the breakdown and recovery of passive film at the sensitized grain boundaries. With the increasing of plastic deformation, the EN transients and AE hits' amplitude are enhanced obviously especially at the final fracture stage. The fractal dimension of sensitized 304 stainless steel in $Na_2S_2O_3$ solution is decreased from 1.9 to 1.0, which indicates that the corrosion type of 304 steel during the stress corrosion cracking process is evolved from intergranular corrosion to crack propagation.The *K*-means cluster results reveal that the extension of brittle intergranular crack and the rupture of ductile bridging ligamentare the two AE sources and attributed to the intergranular stress corrosion cracking of sensitized 304 stainless steel in $Na_2S_2O_3$ solution.

Keywords: stainless steel; intergranular stress corrosion cracking; electrochemical noise; acoustic emission; wavelet fractal dimension; cluster analysis

1. INTRODUCTION

304 stainless steel is widely applied in the nuclear power industry for its excellent mechanical properties and high corrosion resistance. However, the stress corrosion cracking (SCC) of 304 stainless

steel is one of the greatest corrosion problems which occur in the service of pressurized water reactors [1, 2]. Thus the characterization and detection of the SCC behavior of stainless steel has a great practical significance to prevent the failure of structural components of power plants.

As the stress corrosion cracking of metal is resulted from the synergistic effect of mechanical and electrochemical actions of specific metal/environment system, the SCC behavior of materials should be investigated simultaneously from the electrochemical and mechanical aspects. In the electrochemical aspect, electrochemical noise (EN) technique is quite possible to detect and evaluate the corrosion process by the spontaneously generated potential and current fluctuations because of its non-intrusiveness [4]. In 1983, EN technique was firstly applied to detect the SCC behavior of α-brass in 1 M sodium nitrate solution [5].From then on, many studies about the SCC behavior were reported by using EN technique, and the correlation between of SCC behavior and EN parameters under the original signal/transients [6, 7] and statistical analysis [8] was made. In the mechanical aspect, acoustic emission (AE) technique is a non-destructive dynamic testing method to detect the material deformation and corrosion, and the SCC behavior of 304L, 316LN stainless steel were determined by using correlation analysis [9], cluster analysis [3], cumulative parameters analysis [10] and power law model [11] of AE signals. So under the combination of EN and AE techniques the SCC behavior such as the initiation and propagation of cracks could be revealed and characterized [12, 13].

In our previous research, the transgranular stress corrosion cracking behavior of 304 stainless steel in 0.5 mol/L NaCl + 1.5 mol/L H_2SO_4 solution was detected by EN and AE techniques, and the mechanism involving in the transgranular stress corrosion cracking process was discussed by the characterization of EN and AE parameters [3]. The objective of this study is the detection and characterization of intergranular stress corrosion cracking behavior of sensitized 304 stainless steel in $Na_2S_2O_3$ solution by means of EN and AE techniques. The relationship among the fractography, corrosion type and AE sources of intergranular stress corrosion cracking behavior was built, and then the mechanism of intergranular stress corrosion cracking was discussed.

2. EXPERIMENTAL

2.1 Material and heat treatment

304 stainless steel with the composition of 0.080%C, 18.9%Cr, 10.3%Ni, 2.0%Mn, 1.0%Si, 0.045%P, 0.03%S and Fe balance was applied in this experiment. In order to characterize the intergranular stress corrosion cracking behavior, 304 stainless steel was firstly annealed at 1050°C for 1 hour followed by water quenching, and then sensitized at 650°C for 14 hours in a vacuum electric furnace followed by air cooling. After heat treatment, the double loop electrochemical potentiodynamic reactivation test (DL-EPR) was carried out for 304 stainless steel in 0.5mol/L H_2SO_4+0.01mol/L KSCN solution[14]. The degree of sensitization was calculated as 0.53, i.e. 304 stainless steel was heavily sensitized after the above heat treatment.

2.2 Stress corrosion cracking

The intergranular stress corrosion cracking behavior of sensitized 304 stainless steel in 0.5mol/L $Na_2S_2O_3$ solution was evaluated by slow strain rate tensile (SSRT) test on a slow strain rate stress corrosion testing machine with a strain rate of 1×10^{-5} s^{-1} at ambient temperature. The testing specimen was 20mm in the original gauge length, 4mm in width and 2mm in thickness. After fracture, the surface morphology and fractographyof 304 stainless steel were observed by a TDCLS4800 scanning electron microscope.

2.3 Electrochemical noise measurement

Electrochemical noise signals of 304 stainless steel during the SCC process were measured with a sampling frequency of 2Hz by using a home-made system through zero resistance ammeter (ZRA) mode, which described in reference [3]. Three electrodes with an exposed area of 240 mm^2 were made from the same 304 stainless steel, and located in parallel positions with 5mm apart from one another.

After test, the original electrochemical noise signals were firstly processed by a 5-order polynomial fitting to remove the direct current (DC) component. And then the standard deviation of electrochemical potential noise (S_E) and electrochemical current noise (S_I) were calculated, and the noise resistant R_n was calculatedby $R_n=S_E/S_I$ by using statistical analysis method. Meanwhile, the fractal dimension D of electrochemical noise was determined by using wavelet-based fractal analysis method. The details of fractal dimension calculation procedure could be found in Ref.[4,15].

2.4 Acoustic emission measurement

Acoustic emission signals of 304 stainless steel during the SCC process were detected by a μSamos AE system from Physical Acoustics Corporation with two MICRO-80DS AE resonant type piezoelectric sensors, two preamplifiers and a central system. One AE sensor was fixed at the top of the specimen outside the corrosion cell, and the other sensor was located in the bottom of corrosion cell. The amplification was fixed at 40dB with a threshold level of 29dB and sampling frequency of 1MHz. To eliminate electro-magnetic and mechanical disturbances, a high-pass filter with a cut-off frequency of 20 kHz, and a low-pass filter with a cut-off frequency of 400 kHz were used.

After test, the characteristic parametersincluding amplitude, average frequency of AE hits, cumulative hits and cumulative energy of AE signals were obtained and processed by using correlation analysis and *K*-means clustering algorithm methods.

3. RESULTS

3.1 Stress corrosion cracking behavior

Fig. 1 is the stress-time curve of sensitized 304 stainless steel in ambient air and 0.5mol/ L $Na_2S_2O_3$ solution. It can be seen that the sensitized 304 stainless steel in air had the tensile strength of

830MPa and fracture time of 8.5×10^4 s. Whereas the tensile strength and fracture time of 304 stainless steel in 0.5mol /L $Na_2S_2O_3$ solution were only one half and onefifthof that in air respectively. From the loss of tensile strength and fracture time, the stress corrosion cracking susceptibility of sensitized 304 stainless steel in 0.5mol/L $Na_2S_2O_3$ solution was 49.7% and 79.7%, i.e. the stress corrosion cracking of sensitized 304 stainless steel was occurred in 0.5mol/L $Na_2S_2O_3$ solution [16].

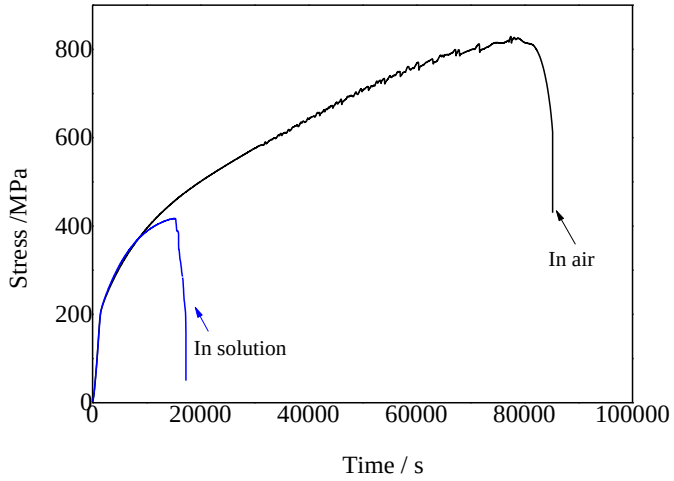

Figure 1. Stress-time curves of sensitized 304 stainless steel in air and 0.5mol/L$Na_2S_2O_3$ solution

The side surface morphology of 304 stainless steel after fracture is shown in Fig. 2. There were several cracks with fewmillimeters in length observed which perpendicular to the tensile direction (Fig. 2a). By further analysis, it was found that all these cracks were in intergranular manner (Fig. 2b). All these results implied that the intergranular stress corrosion cracking was occurred for sensitized 304 stainless steel in 0.5mol/ L $Na_2S_2O_3$ solution.

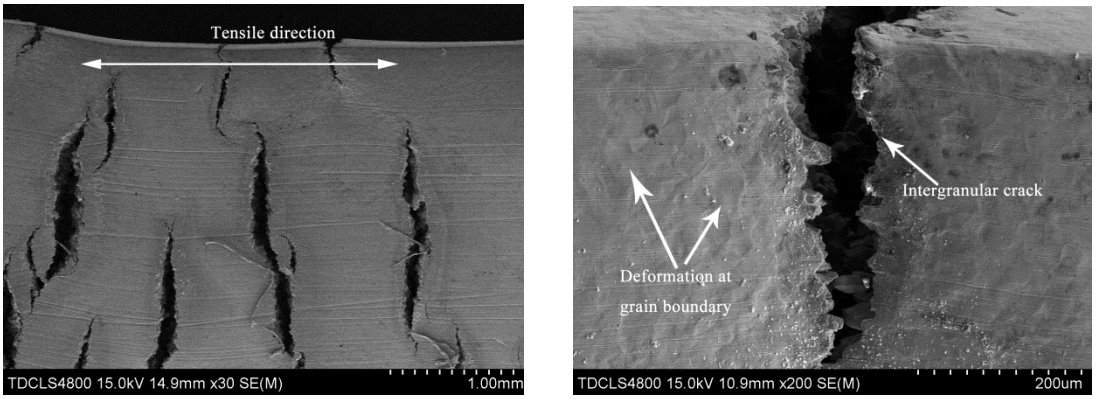

(a)Overall morphology (b) local morphology near intergranular crack

Figure 2. Surface morphology of sensitized 304 stainless steel after SSRT test in 0.5mol/L$Na_2S_2O_3$ solution

Fig. 3 is the fractography of 304 stainless steelin 0.5mol/L $Na_2S_2O_3$ solution. It can be observed that the fractography of 304 stainless steel was composed by eighty percent of intergranular area including several secondary cracks (Fig. 3a and 3b) and twenty percent of ductile area (Fig.3a and Fig.3c). The intergranular aera of steel was in crystalline appearance, and caused by the intergranular stress corrosion cracking of sensitized 304 stainless steel in 0.5mol/L $Na_2S_2O_3$ solution.The ductile area was in bridging liagaments and dimples, and resulted by the overloading on the reduced cross-section in the final tensile stage.

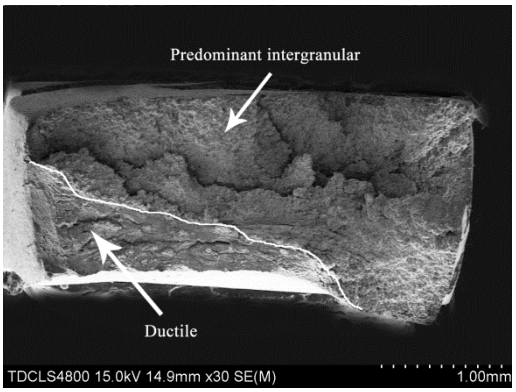

(a) Overall fractrography

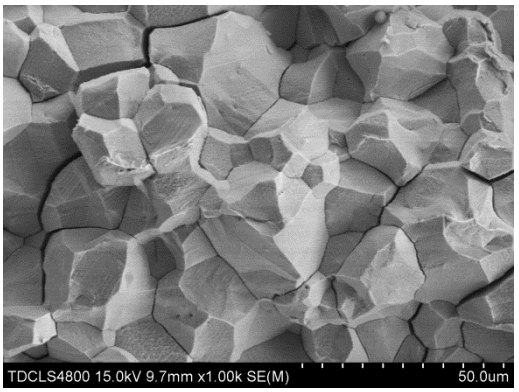

(b) Intergranular area

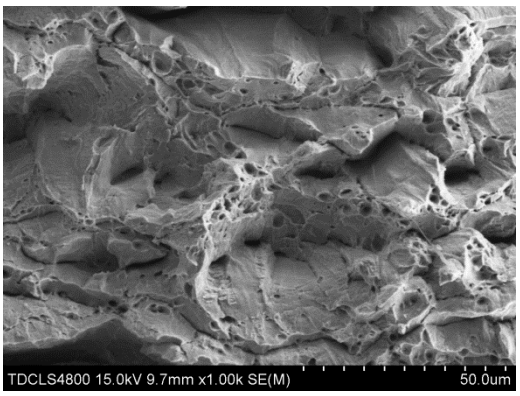

(c) Ductile area

Figure 3. Fractrography of sensitized 304 stainless steel in 0.5mol/L$Na_2S_2O_3$ solution, (a) overall morphology, (b) intergranular area and (c) ductile area

3.3 EN data

Electrochemical noise record and stress-time curve of sensitized 304 stainless steel in $Na_2S_2O_3$ solution are shown in Fig. 4, and the details of EN transients are shown in Fig.5. During the elastic deformation process (Stage 1, before 2000s), there were numerous EN potential and current transients which fluctuated around zero.

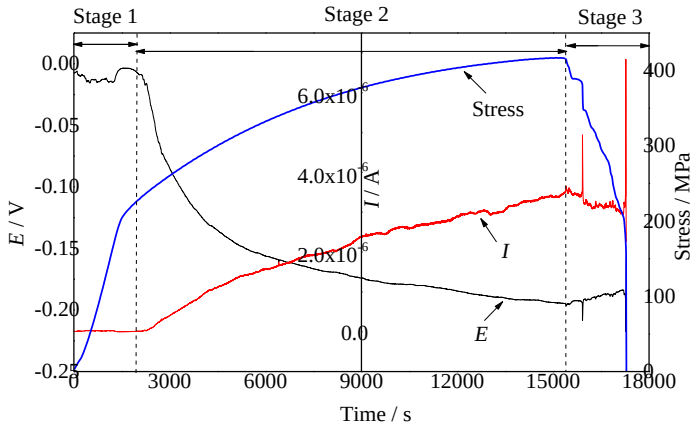

Figure 4. Electrochemical noise record and stress-time curve of sensitized 304 stainless steel in 0.5mol/L$Na_2S_2O_3$ solution

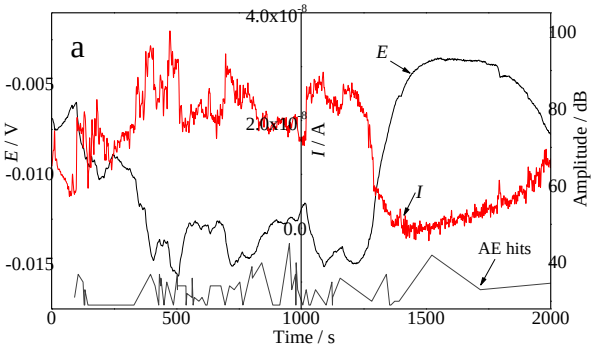

(a) Stage 1

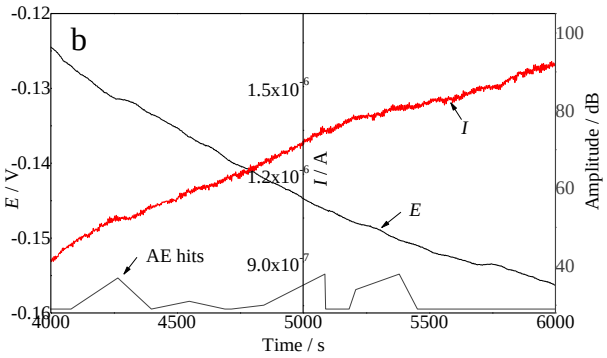

(b)Stage 2

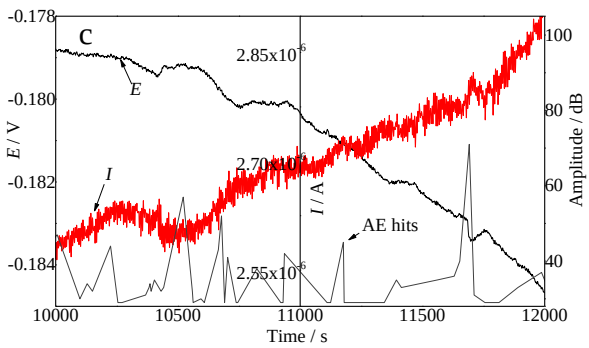

(c) Stage 2

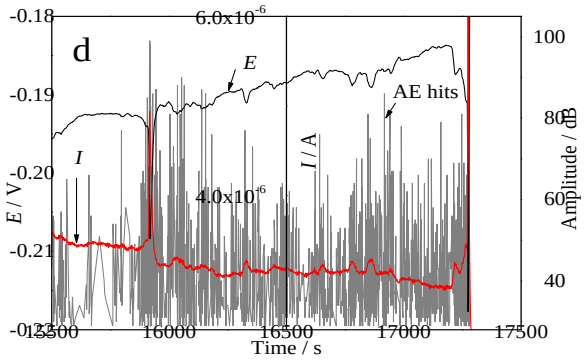

(d) Stage 3

Figure 5. Details of electrochemical noise transient and AE hits' amplitude of sensitized 304 stainless steel in 0.5mol/L$Na_2S_2O_3$ solution in stage 1 (a), stage 2 (b and c) and stage 3 (d)

But the EN potential transients were varied in the opposite direction of EN current transients (Fig.5a). This result implied that there was a repetitive breakdown and recovery of the passive film at corrosion susceptible grain boundaries during the elastic deformation process [8]. It is the film rupture at grain boundaries that the intergranular cracks were formed at the surface of sample, which is accord with the Kovac's result [18].

With the transition from elastic to plastic deformation (Stage 2, 2000-15500s), an abrupt increase in EN current signal and decrease in EN potential signal were detected (Fig.4), which indicated the exposure and enlargement of the new anodic surface due to the plastic deformation. As the time prolonging, EN current signal was increased gradually and EN potential signal was decreased constantly (Fig.5b and Fig.5c). This increase in EN current signal and decrease in EN potential signal were caused by the continuous intergranular crack propagation and ductile bridging ligament rupture [17].

After the formation of neck (Stage 3, 15500-17300s), EN signals showed several sharp transients (Fig.5d). But on the whole, EN current signal was decreased slightly and EN potential signal was increased a little (Fig.4). By correlated with the stress-time curve (Fig.6a) and slope of stress-time curve (Fig.6b), this typical EN current transient with sharp increase and slower decrease had a good correspondence to the slope of stress-time (Fig.6b), i.e. the stress relaxation. As the stress relaxation is corresponded to the ductile fracture due to the rupture of ductile bridging ligament [18, 19], EN transients was caused by the stress relaxation effect or the ductile crack propagation.

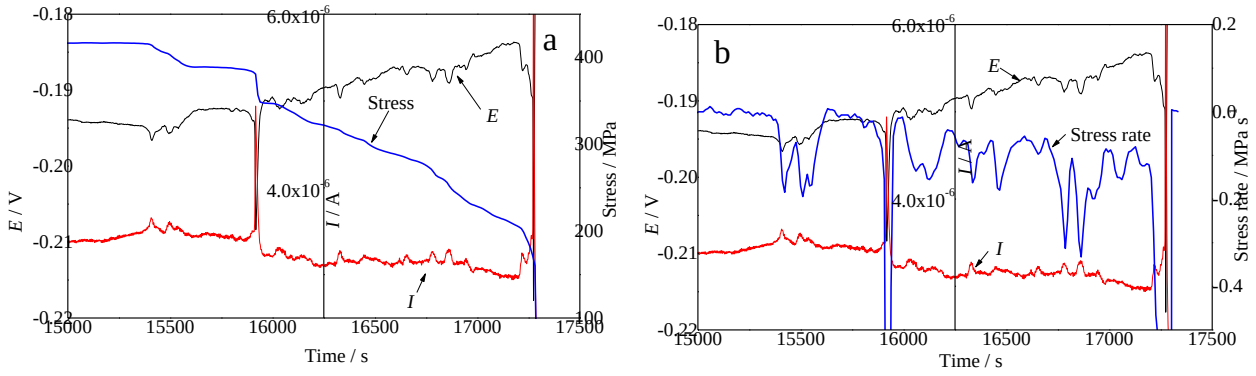

(a)EN vs. stress-time curve (b) EN vs. slope of stress-time curve

Figure 6. Correlation of electrochemical noise transient with stress-time curve (a),and slope of stress-time curve (b) in stage 3

Fig.7 is the electrochemical noise resistance R_n and standard deviation of electrochemical current noise S_I during the SCC process, and the fractal dimension D of 304 stainless steel were calculated and shown in Fig. 8. In the elastic deformation stage, 304 stainless steel has a higher electrochemical noise resistance and a lower standard deviation with a fractal dimension of 1.5-1.9. These results meant that 304 stainless steel was mostly in a passivated state, and the type of corrosion

was intergranular corrosion [4]. As the stress-time curve was evolved into stage 2 and stage 3, the electrochemical noise resistance was decreased obviously to a stable value, and the standard deviation S_I was increased gradually, especially at stage 3. Meanwhile, the fractal dimension was almost kept in a constant around 1.0. These characteristics implied that the corrosion resistance was reduced with the increase of plastic deformation, and the type of corrosion was in a manner ofcrack propagation [4].

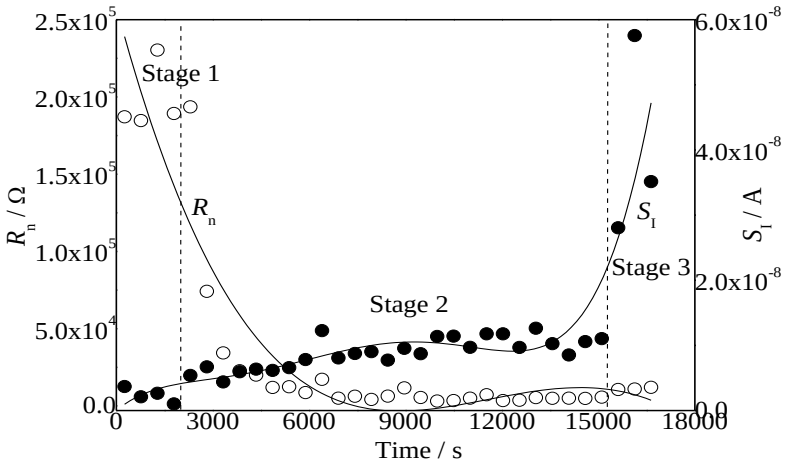

Figure 7. Evolution of R_n and S_I of sensitized 304 stainless steel in 0.5mol/L$Na_2S_2O_3$ solutionwith time

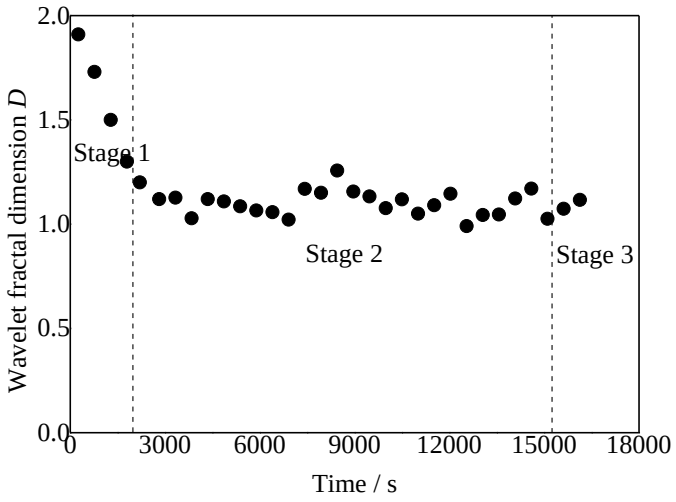

Figure 8. Evolution of wavelet fractal dimension *D*of sensitized 304 stainless steel in 0.5mol/L$Na_2S_2O_3$ solutionwith time

3.4 AE data

The amplitude of acoustic emission hits and stress-time curve ofsensitized 304 stainless steel in $Na_2S_2O_3$ solution are shown in Fig. 9, and the details of AE hits are shown in Fig.5. During the elastic

deformation process (stage 1, before 2000s), a large number of AE hits with amplitude lower than 40dB were observed (Fig.5a and Fig.9). In the first half of plastic deformation (before 9000s), the amplitude was still in lower value (Fig.5b). But in the second half of plastic deformation (9000-15500s), AE hits had a higher amplitude of 60-80dB due to the rupture of ductile bridging ligament (Fig.5c). In the final fracture (stage 3), AE hits with amplitude of 60-100dB was generated (Fig. 5d) [17], which indicated the ductile fracture shown in Fig. 3c was mainly occurred during the last 2000s of the test.

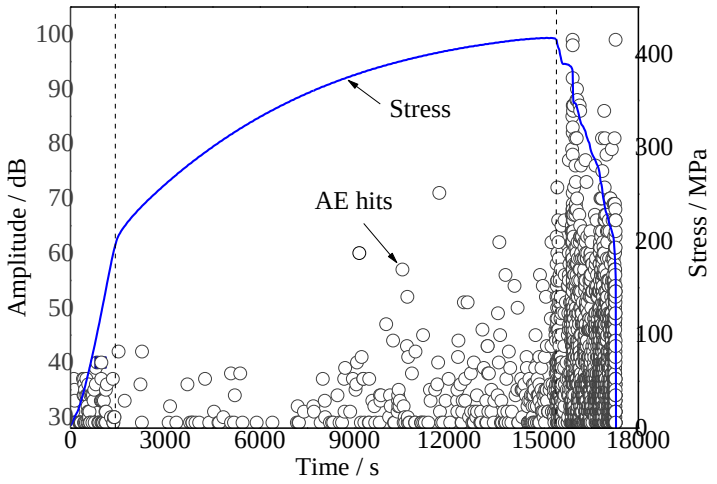

Figure 9. Amplitude of AE hits and stress-time curve of sensitized 304 stainless steel in 0.5mol/L$Na_2S_2O_3$ solution

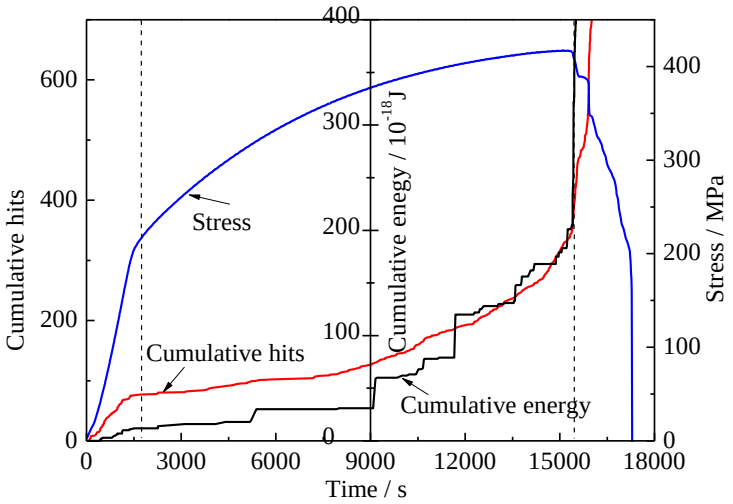

Figure 10. AE cumulative hits, cumulative energy andstress-time curve of sensitized 304 stainless steel in 0.5mol/L$Na_2S_2O_3$ solution

Fig. 10 is the AE cumulative hits and cumulative energy plots of sensitized 304 stainless steel in $Na_2S_2O_3$ solution. It can be seen that three stages could be classified during the IGSCC process. In

stage1, the AE cumulative hits' number and the cumulative energy was in a lower state. In the first half of stage 2, AE cumulative hits number and the cumulative energy was increased slightly, but still in a lower state. In the second half of stage 2 (9000-15500s), AE cumulative hits number was enhanced obviously, and the cumulative energy was increased in a step growth, which meant that the ductile crack was propagated discontinuously. In the final stage, AE cumulative hits number and cumulative energy was increased steeply. Based on the observations in Fig. 2 and Fig. 3 and theexperimental results in references [10, 18], two AE sources might exist in this IGSCC system, namely brittle intergranular crack and ductile bridging ligament rupture. So AE signals could be classified into two clusters, i.e. cluster1is the AE signal from britle intergranular crack, and cluster 2 is the AE signal from ductile fracture.

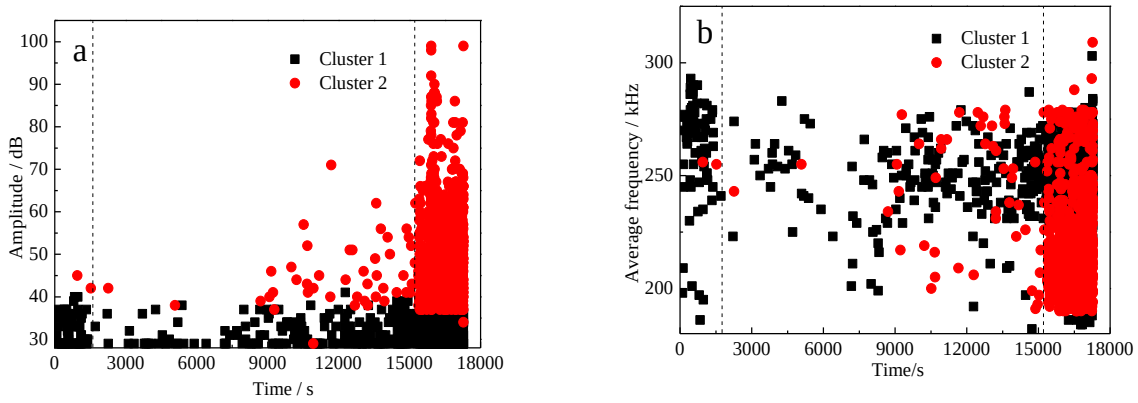

(a) Amplitude vs. time (b) Average frequency vs. time

Figure 11. AE hits' amplitude (a) and average frequency (b) of sensitized 304 stainless steel in 0.5mol/L$Na_2S_2O_3$ solution with time under cluster analysis

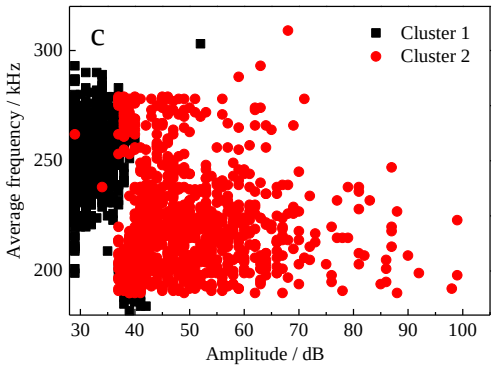

Figure 12. Correlation diagram of AE hits'amplitude with the average frequency of sensitized 304 stainless steel in 0.5mol/L$Na_2S_2O_3$ solution under cluster analysis

Fig.11 is the amplitude and average frequency distribution of AE hits under cluster analysis for sensitized 304 stainless steel in $Na_2S_2O_3$ solution, and the correlation diagram of AE hits amplitude

with the average frequency is shown in Fig.12. AE signals in cluster 1 were distributed in all the IGSCC process with the amplitude lower than 40dB and average frequency of 200~300kHz, while AE signals in cluster 2 were mainly located in the second half of stage 2 and stage 3 with the amplitude higer than 40dB and average frequency of 190~300kHz.The average frequency range of 190~300 kHz is in accordance with the characteristics of crack signal [3, 20], one is generated by brittle intergranular crack and the other is generated by the ductile bridging ligament rupture or ducile frature in the final stage. So these two clusters has almost the same frequency range but different amplitude (Fig. 12) [18]. It is this amplitude difference that these two clusters could be distinguished each other.

4. DISCUSSION

It's well known that the stress corrosion cracking of metal is resulted from the synergistic effect of mechanical and electrochemical actions of specific metal/environment system, and can be divided into three stages, i.e. crack initiation, crack propagation and final failure[21].

In $Na_2S_2O_3$ solution 304 stainless steel is in the passivated state if there is no external stress or deformation applied. Under the elastic deformation, the passive film on sensitized 304 stainless steel especially at the sensitized grain boundaries would be firstly broken down and then re-passivated again [8]. Corresponding this breakdown and recovery of passive film, EN potential signal and current signal were fluctuated around zero and varied in the opposite direction[18], and AE signal was in a lower amplitude due to the lower energy release of passive film rupture (Fig.5a and Fig.10). So in this stage 304 stainless steel has a higher noise resistance R_n, lower current standard deviation S_I (Fig.7)[8] and a intergranular corrosion character (fractal dimension of 1.5-1.9) (Fig.8)[4].

In the plastic deformation stage, the broken passive film could not be re-passivated any more with the increase of plastic deformation, and thus the brittle intergranular cracks were formed and propagated gradually (Fig.2b). Reflected in EN signals, EN current signal was increased positively and EN potential signal was shifted negatively (Fig.5b and Fig.5c)[17]. So the noise resistance R_n was reduced obviously and the current standard deviation S_I was enhanced gradually (Fig.7). In the first half of plastic deformation stage, due to the brittle character of intergranular cracks AE signals had a lower amplitude (Fig.9) and lower cumulative energy (Fig.10)[22]. But with the increasing of plastic deformation, SCC cracks would propagate by the extension of brittle intergranular crack and the rupture of ductile bridging ligament (Fig.11), and thus more AE signals were generated with high amplitude of 60-80dB (Fig.9)[23] and higher cumulative hits and energy (Fig.10).

In the final stage (Stage3), with the formation of neck 304 stainless steel was overloaded and rapidly fractured in a ductile manner (Fig.3a and Fig.3c). So in this stage EN signals were in sharp transients[18,19] and AE signals had a larger amplitude (Fig.5d)[17], the cumulative hits and energy was increased sharply (Fig.10)[24,25], which were caused by the fast rupture of ductile bridging ligament (Fig.3c).

From the above discussion, it can be seen that the crack propagation of sensitized 304 stainless steel in $Na_2S_2O_3$ solution was resulted by the extension of brittle intergranular crack and the rupture of bridging ligament. That's why the fractal dimension of 304 stainless steel in $Na_2S_2O_3$ solution is

around 1.0 (Fig.8), and two AE sources were existed in this intergranular stress corrosion cracking system (Fig.12).

5. CONCLUSIONS

(1) In the elastic deformation process, the small transients in EN and low amplitude of AE hits were related to the breakdown and recovery of passive film at the sensitized grain boundaries.With the increasing of plastic deformation, EN transients and AE hits' amplitude are enhanced obviously especially at the final fracture stage.

(2) The fractal dimension of sensitized 304 stainless steel in $Na_2S_2O_3$ solution is decreased from 1.5-1.9 in the elastic deformation process to 1.0 in the plastic deformation process, which indicates that the corrosion type of 304 steel during the stress corrosion cracking process is evolved from intergranular corrosion to crack propagation.

(3) The extension of brittle intergranular crack and the rupture of ductile bridging ligament are the two AE sources and attributed to the intergranular stress corrosion cracking of sensitized 304 stainless steel in $Na_2S_2O_3$ solution.

ACKNOWLEDGEMENTS
This paper was supported by Key Project of Tianjin Natural Science Foundation (13JCZDJC29500) and Specialized Research Fund for the Doctoral Program of Higher Education (20120032110029), and National Key Basic Research Program of China (No.2014CB046801).

References

1. R.N. Parkins, P.M. Singh, *Corrosion*, 46(6) (1990) 485-499.
2. M. LEBAN, Ž.BAJT, A. LEGAT,*Electrochimica Acta*, 49(17/18) (2004) 2795-2801.
3. G. Du, J. Li, W. K. Wang, X. Jiang and S. Z. Song, *Corros. Sci.*, 53(9) (2011) 2918-2926.
4. X. H. Wang, J. H. Wang, C. W. Fu and Y. K. Gao, *Int. J. Electrochem. Sci.*, 8(5) (2013) 7211-7222.
5. R. C. Newman and K. Sieradzki, *Scripta Metallurgica*, 17 (5) (1983) 621-624.
6. M. Leban, V. Doleček and A. Legat, *Corrosion*, 56 (9) (2000) 921-927.
7. Y. Watanabe and T. Kondo, *Corrosion*, 56 (12) (2000) 1250-1255.
8. T. Anita, M. G. Pujar, H. Shaikh, R. K. Dayal and H. S. Khatak, *Corros. Sci.*, 48 (9) (2006) 2689-2710.
9. K. Máthis, D. Prchal, R. Novotný and P. Hähner, *Corros. Sci.*, 53 (1) (2011) 59-63.*Sci.*, 49 (2) (2007) 740-765.
10. H. Shaikh, R. Amirthalingam, T. Anita, N. Sivaibharasi, T. Jaykumar, P. Manohar and H. S. Khatak, *Corros. Sci.*, 49 (2) (2007) 740-765.
11. M. G. Alvarez, P. Lapitz and J. Ruzzante, *Corros. Sci.*, 55(1) (2012) 5-9.
12. A. Yonezu, H. Choand M. Takemoto,*Meas. Sci. Technol*, 17 (2006) 2447-2454.
13. J. Kovač, M. LebanandA. Legat, *Materials and Corrosion*, 58(12) (2007) 970-976.
14. P. Muri, F.V. Sousa, K.S. Assis, A.C. Rocha, O.R. Mattos,I.C.P. Margarit-Mattos, *Electrochimica Acta*, 124 (2014) 183-189.

15. X.F. Liu, H.G. Wang, H.C. Gu, *Corros. Sci*,48 (2006) 1337-1367.
16. A. Abou-Elazm, R. Abdel-Karim, I. Elmahallawi, R. Rashad, *Corros Sci*, 51(2) (2009) 203-208.
17. J. Kovač, M. Leban and A. Legat, *Electrochim. Acta*, 52 (27) (2007) 7607-7616.
18. J. Kovac, C. Alaux, T. J. Marrow, E. Govekar and A. Legat, *Corros. Sci.*, 52 (6) (2010) 2015-2025.
19. M. Breimesser, S. Ritter, H. P. Seifert, T. Suter and S. Virtanen, *Corros. Sci.*, 63 (0) (2012) 129-139.
20. S. Ramadan, L. Gaillet, C. Tessier and H. Idrissi, *Appl. Surf. Sci.*, 254 (8) (2008) 2255-2261.
21. N. A. Vu, A. Castel, R. François, *Corros. Sci*., 51 (2009) 1453-1459.
22. K. Máthis, D. Prchal, R. Novotny, P. Hähner, *Corros. Sci*., 53 (2011) 59-63.
23. M.G. Alvarez, P. Lapitz, J. Ruzzante， *Corros. Sci*., 50 (2008) 3382-3388.
24. V. Smanio, M. Fregonese, J. Kittel, T. Cassagne, F. Ropital, B. Normand, *Corros. Sci*., 53 (2011) 3942-3949.
25. H. Shaikh, R. Amirthalingam, T. Anita, N. Sivaibharasi, T. Jaykumar, P. Manohar, H.S. Khatak, *Corros. Sci*., 49 (2007) 740-765.